Control of Parallel Three-Phase PWM Converters Under Generalized Unbalanced Operating Conditions

Xueguang Zhang, *Member, IEEE*, Zhichao Fu, Yi Xiao, Gaolin Wang, *Member, IEEE*, and Dianguo Xu, *Senior Member, IEEE*

***Abstract*—This paper proposes a new control scheme for parallel three-phase pulse width modulation converters under generalized unbalanced operating conditions. An average model of the parallel system in positive-sequence synchronous reference frame is derived to analyze the influence of generalized unbalanced operating conditions in ac side. It is seen that the unbalance factors in filter inductance will not only give rise to negative-sequence circulating current, but also contribute to generating zero-sequence circulating current (ZSCC). The negative-sequence circulating current can be inhibited by suppressing the negative-sequence components in ac output currents of parallel modules with a proportional integral resonant (PIR) controller. An improved feed-forward strategy and a PIR controller for ZSCC control are proposed for unbalanced operating conditions. The disturbances in ZSCC caused by unbalance factors in filter inductance can be rejected with feed-forward strategy. Because the disturbance in ZSCC is the fluctuation in grid frequency which can be suppressed by a resonance controller, therefore, a PIR controller is adopted in ZSCC controller. The proposed scheme can effectively suppress the circulating currents between the parallel modules and as a result, the distortions in output currents can be greatly reduced. Experimental results confirm the performance and effectiveness of the proposed method.**

***Index Terms*—Circulating currents control, feed-forward, generalized unbalanced operating conditions, negative-sequence circulating current, parallel three-phase pulse width modulation (PWM) converters, proportional integral resonant (PIR) controller.**

I. Introduction

A THREE-PHASE pulse width modulation (PWM) converter has been widely employed in distributed generation systems [1]–[3] owing to its advanced features, and its parallel connection topology is becoming popular used to increasing the power rating of distributed generation systems due to its simplicity, low cost, and high flexibility. However, these features are not necessarily achieved when the converters are directly connected between common dc and ac buses under generalized operating conditions of unbalanced grid supply and unbalanced ac filter inductance. The main concern in a parallel system is the currents circulating between the parallel modules [4], [5].

The zero-sequence component in circulating currents is the major problem under balanced operating conditions, the relationships between switching pattern and zero-sequence circulating current (ZSCC) is analyzed in detail by [6]. To reduce the ZSCC, special PWM techniques have been proposed. The discontinuous space modulation based interleaved PWM method would effectively reduce the circulating current with a power-factor-correction circuit, whereas it will result in high current ripple in parallel modules [7]. Instead, a harmonic elimination PWM method proposed by [8] can overcome the current ripple disadvantage and effectively eliminate both the high-frequency and low-frequency components in ZSCC. However, it suffers from high-switching losses. A multicarrier PWM modulation technique without using zero vectors is proposed to mitigate the ZSCC [9]. The ZSCC can be suppressed to some extent by reducing the common-mode voltage. An average model of the parallel converters in rotating coordinates is introduced in [10], instead of avoiding using zero vectors, the popular space vector pulse width modulation (SVPWM) modulation technique can effectively suppress the zero-sequence component in circulating current by adjusting the distribution of two zero vectors in each PWM cycle with a proportional integral (PI) controller [11]. However, the traditional PI method cannot effectively rejects the disturbances caused by unbalance factors in filter inductance. Nonlinear control methods were also presented to resist the circulating current [12], but the algorithms are too complicated to implement.

The operation of three-phase PWM converter in unbalanced condition has been widely researched [13]–[17], but the operation of paralleled converters has not been paid much attention. The mechanism of circulating currents has been analyzed in pervious works [18], [19]. Apart from zero-sequence component in circulating currents, unbalanced grid supply would probably generate negative-sequence circulating current between parallel modules. The negative-sequence and zero-sequence components can both be effectively eliminated by isolating transformers as the circulating currents paths are made open circuits [20]. But in return, the parallel system will become costly and bulky. Similar problems will be encountered by using separated dc supply [21]. For parallel systems with both common dc-link and ac bus to reduce costs and size, interphase reactors may be used to provide high impedance for circulating currents [22]. As a matter of fact, the negative-sequence circulating current is generated mainly because of the negative-sequence components in output currents of the parallel modules. Thus,

Manuscript received July 17, 2015; revised November 17, 2015 and March 27, 2016; accepted May 22, 2016. Date of publication June 7, 2016; date of current version January 20, 2017. This work was supported by the National Natural Science Foundation of China under Grants 51107020, 51237002, and 51577040. This work was also sponsored by grants from the Power Electronics Science and Education Development Program of Delta Environmental and Educational Foundation. Recommended for publication by Associate Editor A. Trzynadlowski.

The authors are with the Department of Electrical Engineering, Harbin Institute of Technology, Harbin, Heilongjiang 150001, China (e-mail: zxghit@126.com; fzcsd92@163.com; xiaoyihust@163.com; wgl818@hit.edu.cn; xudiang@hit.edu.cn).

Color versions of one or more of the figures in this paper are available online at http://ieeexplore.ieee.org.

Digital Object Identifier 10.1109/TPEL.2016.2577560

coordinate control method has been proposed in and [19] to inhibit the negative-sequence circulating current by suppressing the negative-sequence components in currents. Because of the capability of achieving zero steady-state error at ac frequency, resonant controller is now used in the ac system, especially for grid current control in PWM converter system [23]–[25], but its application for circulating current control has not been published.

Compared to the work of [26], a new control scheme for the parallel three-phase PWM converters under generalized operating conditions was proposed. An average model of the parallel system in positive-sequence synchronous reference frame (PSRF) is derived to analyze the influence of unbalanced operating conditions on converter output currents in ac side. The unbalanced grid supply would cause negative-sequence components in the output currents and may also result in negative-sequence circulating current. A proportional integral resonant (PIR) controller is adopted to inhibit the negative-sequence circulating current by suppressing the negative-sequence components in output currents. Moreover, it is found that the unbalance factors in filter inductance will not only give rise to the generating of negative-sequence circulating current, but also make disturbances to the ZSCC system, which will contribute to generating low-frequency components in ZSCC. Besides, to reject the disturbances caused by unbalance factors in filter inductance to ZSCC system, improved zero-vector feed-forward method can be used. Because the feed-forward method relies on the parameter of filter inductance, and the ZSCC caused by unbalance filter is normally in grid frequency, so a resonance controller in grid frequency can be used. Combined with the conventional PI controller, a PIR controller in grid frequency for ZSCC control is adopted in this paper. Improved suppression performance can be achieved with the proposed scheme and the distortions in output currents can be greatly reduced. The feasibility and advantage of the proposed scheme are verified through experimental analysis.

The remainder of the paper is organized as follows. In Section II, the definition of circulating currents and its zero-sequence component is presented and an average model of parallel three-phase converters under generalized unbalanced operating conditions is derived in PSRF. In Section III, the influence of unbalance factors in filter inductance on the active–reactive current system and ZSCC control system is analyzed. The principle of proposed circulating current strategy based on feed-forward method and PIR controller is introduced in detail. Section IV presents the experimental results and Section V concludes the paper.

II. Model of Parallel Three-Phase Converters Unbalanced Operating Conditions

The parallel structure of three-phase boost-type PWM converters is shown in Fig. 1. The common dc-link converter modules are connected to the ac grid through filter inductance. As a result, the circulating currents paths are formed due to the fact that the switches in different modules are connected in series. In general, there exist two types of circulating currents paths, i.e., the ZSCC paths and nonzero-sequence circulating current paths. The ZSCC paths, take phase *a,* for example, can

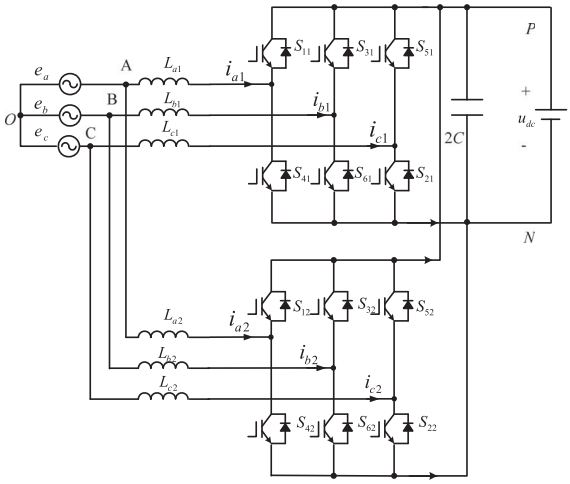

Fig. 1. Topology structure of parallel connection system of three-phase PWM converter.

be listed as $\mathrm{A}-L_{\mathrm{a1}}-\mathrm{S11}-\mathrm{P}-\mathrm{N}-\mathrm{S42}-L_{\mathrm{a2}}-\mathrm{A}$ and $\mathrm{A}-L_{\mathrm{a2}}-\mathrm{S12}-\mathrm{P}-\mathrm{N}-\mathrm{S41}-L_{\mathrm{a1}}-\mathrm{A}$. This type of circuits are formed by two switches and inductances in the same phase of different converters, the dc bus voltage is the only electromotive force contained in the circuits. In contrast, the nonzero-sequence circulating current paths, for instance, $\mathrm{O}-\mathrm{A}-L_{\mathrm{a1}}-\mathrm{S11}-\mathrm{P}-\mathrm{N}-\mathrm{S62}-L_{\mathrm{b2}}-\mathrm{B}-\mathrm{O}, \mathrm{O}-\mathrm{A}-L_{\mathrm{a2}}-\mathrm{S12}-\mathrm{P}-\mathrm{N}-\mathrm{S61}-L_{\mathrm{b1}}-\mathrm{B}-\mathrm{O}, \mathrm{O}-\mathrm{B}-L_{\mathrm{b2}}-\mathrm{S32}-\mathrm{P}-\mathrm{N}-\mathrm{S41}-L_{\mathrm{a1}}-\mathrm{A}-\mathrm{O}, \mathrm{O}-\mathrm{B}-L_{\mathrm{b1}}-\mathrm{S31}-\mathrm{P}-\mathrm{N}-\mathrm{S42}-L_{\mathrm{a2}}-\mathrm{A}-\mathrm{O}$ contain two more ac phase voltages.

Generally, in practical applications, while modular converters are usually designed to have equal values of parameters, tolerance in parameter dispersion is very common, especially in the line inductance [27], [28]. As a consequence, the values of three-phase filter inductance are not strictly equal, which will lead to asynchronous actions in switches, and consequently, circulating currents will be generated. Circulating current in phase $k(k = a, b, c)$ of converter 1 can be defined as

$$i_{\mathrm{ck}} = \frac{i_{k1} - i_{k2}}{2}. \tag{1}$$

And the zero-sequence component in the circulating currents, which is the major concern under balanced conditions, can be defined as

$$i_{\mathrm{zx}} = (i_{\mathrm{ax}} + i_{\mathrm{bx}} + i_{\mathrm{cx}})/3 \tag{2}$$

where $x = 1, 2$ is the number of the parallel modules. The nonzero-sequence component in the circulating currents usually can be neglected under balanced conditions as output currents of the parallel modules are balanced. However, this is not necessarily true under the operating conditions of unbalanced grid voltage and unbalanced ac filter inductance. Such a generalized unbalance condition is quite common in application and will result in appearance of negative-sequence as well as odd harmonic components in the output currents, which would distort the output currents of parallel systems. The negative-sequence currents will probably contribute to generating nonzero-sequence component in circulating currents, and here, we refer it to negative-sequence circulating current.

To analyze the influence of unbalance conditions on circulating currents, an analytic model of the parallel system should be derived. Choose the dc negative side as a reference point, then from Kirchhoff's voltage, the parallel structure under generalized unbalanced operating conditions can be described by the following differential equation as:

$$\begin{cases} L_{\mathrm{ax}}\dfrac{di_{\mathrm{ax}}}{dt} = e_a - d_{\mathrm{ax}}u_{\mathrm{dc}} + u_{\mathrm{ON}} \\ L_{\mathrm{bx}}\dfrac{di_{\mathrm{bx}}}{dt} = e_b - d_{\mathrm{bx}}u_{\mathrm{dc}} + u_{\mathrm{ON}} \\ L_{\mathrm{cx}}\dfrac{di_{\mathrm{cx}}}{dt} = e_c - d_{\mathrm{cx}}u_{\mathrm{dc}} + u_{\mathrm{ON}} \end{cases} \tag{3}$$

where L_{kx}, i_{kx}, and d_{kx} $(k = a, b, c, x = 1, 2)$ are the filter inductance, current, and the duty ratio of the top switch in phase k of converter x, respectively. To simplify the analysis, the resistor of the filter is neglected. In general terms, the grid fundamental frequency voltage under unbalanced conditions can be expressed as

$$\begin{bmatrix} e_a \\ e_b \\ e_c \end{bmatrix} = E_{\mathrm{pm}} \begin{bmatrix} \cos\omega t \\ \cos\left(\omega t - \dfrac{2}{3}\pi\right) \\ \cos\left(\omega t + \dfrac{2}{3}\pi\right) \end{bmatrix} + E_{\mathrm{nm}} \begin{bmatrix} \cos\omega t \\ \cos\left(\omega t + \dfrac{2}{3}\pi\right) \\ \cos\left(\omega t - \dfrac{2}{3}\pi\right) \end{bmatrix} \tag{4}$$

where ω is the grid fundamental angular frequency, E_{pm} and E_{nm} are the amplitudes of positive-sequence and negative-sequence voltages, respectively. Conventionally, the ac variable can be transformed into the PSRF with a three-dimensional nonsingular matrix as

$$\boldsymbol{x}_{\mathbf{dqz}} = \boldsymbol{T}_{\boldsymbol{s-r}}.\boldsymbol{x}_{\mathbf{abc}} \tag{5}$$

where $\boldsymbol{x}_{\mathbf{abc}}$ and $\boldsymbol{x}_{\mathbf{dqz}}$ represent the ac variable and its transformed variable in PSRF, respectively. The components x_d, x_q, and x_z are referred to active, reactive, and zero-sequence components of $\mathbf{x}_{\mathrm{dqz}}$ in PSRF, the transformation matrix is expressed as

$$\boldsymbol{T}_{\mathbf{s-r}} = \frac{2}{3}\begin{bmatrix} \cos\omega t & \cos(\omega t - 2\pi/3) & \cos(\omega t + 2\pi/3) \\ -\sin\omega t & -\sin(\omega t - 2\pi/3) & -\sin(\omega t + 2\pi/3) \\ \dfrac{1}{2} & \dfrac{1}{2} & \dfrac{1}{2} \end{bmatrix}.$$

Therefore, from (3) to (5), the parallel structure under generalized operating conditions can be described can be in PSRF expressed as

$$\begin{cases} \left(L_{\mathrm{mx}} + \dfrac{1}{3}L_{\cos 2\mathrm{nx}}\right)\dfrac{di_{\mathrm{dx}}}{dt} - \dfrac{\omega}{3}L_{\sin 2\mathrm{nx}}i_{\mathrm{dx}} - \dfrac{L_{\sin 2\mathrm{nx}}}{3}\dfrac{di_{\mathrm{qx}}}{dt} \\ -\omega\left(L_{\mathrm{mx}} + \dfrac{1}{3}L_{\cos 2\mathrm{nx}}i_{\mathrm{qx}}\right) + \dfrac{2L_{\cos \mathrm{px}}}{3}\dfrac{di_{\mathrm{zx}}}{dt} = \tilde{e_d} - u_{\mathrm{dx}} \\ \left(L_{\mathrm{mx}} - \dfrac{1}{3}L_{\cos 2\mathrm{nx}}\right)\dfrac{di_{\mathrm{qx}}}{dt} + \dfrac{\omega L_{\sin 2\mathrm{nx}}}{3}i_{\mathrm{qx}} - \dfrac{L_{\sin 2\mathrm{nx}}}{3}\dfrac{di_{\mathrm{dx}}}{dt} \\ +\omega\left(L_{\mathrm{mx}} - \dfrac{1}{3}L_{\cos 2\mathrm{nx}}\right)i_{\mathrm{dx}} - \dfrac{2L_{\sin \mathrm{px}}}{3}\dfrac{di_{\mathrm{zx}}}{dt} = \tilde{e_q} - u_{\mathrm{qx}} \\ \dfrac{L_{\cos \mathrm{px}}}{3}\dfrac{di_{\mathrm{dx}}}{dt} - \dfrac{\omega L_{\sin \mathrm{px}}}{3}i_{\mathrm{dx}} - \dfrac{L_{\sin \mathrm{px}}}{3}\dfrac{di_{\mathrm{qx}}}{dt} \\ -\dfrac{\omega L_{\cos \mathrm{px}}}{3}i_{\mathrm{qx}} + L_{\mathrm{mx}}\dfrac{di_{\mathrm{zx}}}{dt} = -u_{\mathrm{zx}} \end{cases} \tag{6}$$

$$\begin{aligned} L_{\mathrm{mx}} &\triangleq (L_{\mathrm{ax}} + L_{\mathrm{bx}} + L_{\mathrm{cx}})/3 \\ L_{\cos 2nx} &\triangleq L_{\mathrm{ax}}\cos 2\,\omega t + L_{\mathrm{bx}}\cos(2\,\omega t + 2\pi/3) \\ &\quad + L_{\mathrm{cx}}\cos(2\,\omega t - 2\pi/3) \\ L_{\sin 2nx} &\triangleq L_{\mathrm{ax}}\sin 2\,\omega t + L_{\mathrm{bx}}\sin(2\,\omega t + 2\pi/3) \\ &\quad + L_{\mathrm{cx}}\sin(2\,\omega t - 2\pi/3) \\ L_{\cos px} &\triangleq L_{\mathrm{ax}}\cos\omega t + L_{\mathrm{bx}}\cos(\omega t - 2\pi/3) \\ &\quad + L_{\mathrm{cx}}\cos(\omega t + 2\pi/3) \\ L_{\sin px} &\triangleq L_{\mathrm{ax}}\sin\omega t + L_{\mathrm{bx}}\sin(\omega t - 2\pi/3) \\ &\quad + L_{\mathrm{cx}}\sin(\omega t + 2\pi/3) \\ \tilde{e}_d &= E_{\mathrm{pm}} + E_{\mathrm{nm}}\cos 2\,\omega t \\ \tilde{e}_q &= -E_{\mathrm{nm}}\cos 2\,\omega t \\ u_{\mathrm{dx}} &= \left(d_{\mathrm{ax}}\cos\omega t + d_{\mathrm{bx}}\cos\left(\omega t - \frac{2\pi}{3}\right)\right. \\ &\quad \left. + \; d_{\mathrm{cx}}\cos\left(\omega t + \frac{2\pi}{3}\right)\right)u_{\mathrm{dc}} = d_{\mathrm{dx}}u_{\mathrm{dc}} \\ u_{\mathrm{qx}} &= \left(-d_{\mathrm{ax}}\sin\omega t - d_{\mathrm{bx}}\sin\left(\omega t - \frac{2\pi}{3}\right)\right. \\ &\quad \left. - \; d_{\mathrm{cx}}\sin\left(\omega t + \frac{2\pi}{3}\right)\right)u_{\mathrm{dc}} = d_{\mathrm{qx}}u_{\mathrm{dc}} \\ u_{\mathrm{zx}} &= (d_{\mathrm{ax}} + d_{\mathrm{bx}} + d_{\mathrm{cx}})u_{\mathrm{dc}}/3 = d_{\mathrm{zx}}u_{\mathrm{dc}}. \end{aligned}$$

A. Model of the Active–Reactive Current System

It should be noted that coupling exist between the zero-sequence current system and the active–reactive current system. A precise model of the active–reactive current system is often favorable when designing current controllers. Based on the consideration, the active–reactive current system can be derived from (6) as the following form:

$$\begin{cases} \left(L_{\mathrm{mx}} + \dfrac{1}{3}L_{\cos 2\mathrm{nx}} - \dfrac{2L_{\cos \mathrm{px}}^2}{9L_{\mathrm{mx}}}\right)\dfrac{di_{\mathrm{dx}}}{dt} \\ +\omega\left(L_{\mathrm{mx}} + \dfrac{1}{3}L_{\cos 2\mathrm{nx}} + \dfrac{2L_{\cos \mathrm{px}}^2}{9L_{\mathrm{mx}}}\right)i_{\mathrm{qx}} \\ +\left(\dfrac{2L_{\sin \mathrm{px}}L_{\cos \mathrm{px}}}{9L_{\mathrm{mx}}} - \dfrac{L_{\sin 2\mathrm{nx}}}{3}\right)\dfrac{di_{\mathrm{qx}}}{dt} \\ +\omega\left(\dfrac{2L_{\sin \mathrm{px}}L_{\cos \mathrm{px}}}{9L_{\mathrm{mx}}} - \dfrac{L_{\sin 2\mathrm{nx}}}{3}\right)i_{\mathrm{dx}} \\ = \tilde{e_d} - u_{\mathrm{dx}} + \dfrac{2L_{\cos \mathrm{px}}}{3L_{\mathrm{mx}}}u_{\mathrm{zx}} \\ \left(L_{\mathrm{mx}} - \dfrac{1}{3}L_{\cos 2\mathrm{nx}} - \dfrac{2L_{\sin \mathrm{px}}^2}{9L_{\mathrm{mx}}}\right)\dfrac{di_{\mathrm{qx}}}{dt} \\ +\omega\left(L_{\mathrm{mx}} - \dfrac{1}{3}L_{\cos 2\mathrm{nx}} - \dfrac{2L_{\sin \mathrm{px}}^2}{9L_{\mathrm{mx}}}\right)i_{\mathrm{dx}} \\ +\left(\dfrac{2L_{\sin \mathrm{px}}L_{\cos \mathrm{px}}}{9L_{\mathrm{mx}}} - \dfrac{L_{\sin 2\mathrm{nx}}}{3}\right)\dfrac{di_{\mathrm{dx}}}{dt} \\ +\omega\left(\dfrac{L_{\sin 2\mathrm{nx}}}{3} - \dfrac{2L_{\sin \mathrm{px}}L_{\cos \mathrm{px}}}{9L_{\mathrm{mx}}}\right)i_{\mathrm{qx}} \\ = \tilde{e_q} - u_{\mathrm{qx}} - \dfrac{2L_{\sin \mathrm{px}}}{3L_{\mathrm{mx}}}u_{\mathrm{zx}} \end{cases}. \tag{7}$$

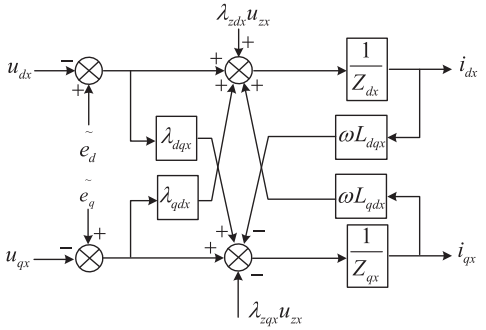

Fig. 2. Active–reactive current system in PSRF under generalized unbalanced operating conditions.

In practical applications, the tolerable difference in filter inductance between its real value and nominal is often about $\pm 10\%$, even under severe environment, the difference could be limited to an acceptable range. Thus, by omitting the negligible high-order terms in (7), the mathematical model of active–reactive can be finally obtained as

$$\begin{cases} \left(L_{\mathrm{mx}} + \dfrac{1}{3}L_{\cos 2\mathrm{nx}}\right)\dfrac{di_{\mathrm{dx}}}{dt} - \omega\left(L_{\mathrm{mx}} + \dfrac{1}{3}L_{\cos 2\mathrm{nx}}\right)i_{\mathrm{qx}} \\ = \tilde{e_d} - u_d + \dfrac{L_{\sin 2n}}{3L_{\mathrm{mx}} - L_{\cos 2\mathrm{nx}}}(\tilde{e_q} - u_q) + \dfrac{2L_{\cos \mathrm{px}}}{3L_{\mathrm{mx}} - L_{\cos 2\mathrm{nx}}}u_{\mathrm{zx}} \\ \left(L_{\mathrm{mx}} - \dfrac{1}{3}L_{\cos 2\mathrm{nx}}\right)\dfrac{di_{\mathrm{qx}}}{dt} + \omega\left(L_{\mathrm{mx}} - \dfrac{1}{3}L_{\cos 2\mathrm{nx}}\right)i_{\mathrm{dx}} \\ = \dfrac{L_{\sin 2\mathrm{nx}}}{3L_{\mathrm{mx}} + L_{\cos 2\mathrm{nx}}}(\tilde{e_d} - u_d) + \tilde{e_q} - u_q - \dfrac{2L_{\sin \mathrm{px}}}{3L_{\mathrm{mx}} - L_{\cos 2\mathrm{nx}}}u_{\mathrm{zx}} \end{cases} \tag{8}$$

where L_{mx} is the average value of three-phase inductance, $L_{\cos 2\mathrm{nx}}$, $L_{\cos \mathrm{px}}$, and $L_{\sin 2\mathrm{nx}}$, $L_{\sin \mathrm{px}}$ are the cosine and sine terms of the unbalanced filter inductance in parallel modules with $2\,\omega$ and ω frequency, respectively. While $\tilde{e_d}$, $\tilde{e_q}$ represent the active and reactive components of unbalanced grid voltage in PSRF and u_{zx} is the zero-sequence component in output voltage.

Define $Z_{\mathrm{dx}} = (L_{\mathrm{mx}} + \frac{1}{3}L_{\cos 2\mathrm{nx}})p$, $Z_{\mathrm{qx}} = (L_{\mathrm{mx}} - \frac{1}{3}L_{\cos 2\mathrm{nx}})p$, where p is the differential operator, and $L_{\mathrm{qdx}} = L_{\mathrm{mx}} + \frac{1}{3}L_{\cos 2\mathrm{nx}}$, $L_{\mathrm{dqx}} = L_{\mathrm{mx}} - \frac{1}{3}L_{\cos 2\mathrm{nx}}$, $\lambda_{\mathrm{qdx}} = \frac{L_{\sin 2n}}{3L_{\mathrm{mx}} - L_{\cos 2\mathrm{nx}}}$, $\lambda_{\mathrm{dqx}} = \frac{L_{\sin 2\mathrm{nx}}}{3L_{\mathrm{mx}} + L_{\cos 2\mathrm{nx}}}$, $\lambda_{\mathrm{zdx}} = \frac{2L_{\cos \mathrm{px}}}{3L_{\mathrm{mx}} - L_{\cos 2\mathrm{nx}}}$, $\lambda_{\mathrm{zqx}} = \frac{2L_{\sin \mathrm{px}}}{3L_{\mathrm{mx}} - L_{\cos 2\mathrm{nx}}}$ as the coupling coefficients inside the active–reactive current system and between the active–reactive current system and ZSCC system. Then, the diagram of active–reactive current system can be obtained as Fig. 2.

It is interesting to note that the unbalance factors in filter inductance will lead oscillatory components with an angular frequency of $2\,\omega$ to the line impedance in PSRF. Besides, similar oscillatory terms will also appear in grid voltage components $\tilde{e}_d$ $\tilde{e}_q$ due to the existence of negative-sequence component in grid voltage. Additionally, when the popular SVPWM modulation technique is adopted, the zero-sequence output voltage at ac side in the parallel modules will be a triangular voltage with an angular frequency of $3\,\omega$[29], and this in return, will also produce $2\,\omega$ oscillatory components in the active–reactive current system. Unfortunately, all these oscillatory terms will give rise to negative-sequence currents in parallel modules.

Generally, the negative-sequence currents will result in unbalanced output currents and cause different switching losses in three bridges of a single converter. Moreover, it will probably cause negative-sequence component in circulating currents. According to the theory depicted in [18], the negative-sequence circulating current under generalized unbalanced operating conditions can be expressed as

$$i_{\mathrm{cn}} = \frac{1}{6}\begin{bmatrix} \left(\dfrac{e_a - u_{\mathrm{NO}} - d_{a1}u_{\mathrm{dc}}}{Z_{a1}} + \alpha^2\dfrac{e_b - u_{\mathrm{NO}} - d_{b1}u_{\mathrm{dc}}}{Z_{b1}} + \alpha\dfrac{e_c - u_{\mathrm{NO}} - d_{c1}u_{\mathrm{dc}}}{Z_{c1}}\right) \\ -\left(\dfrac{e_a - u_{\mathrm{NO}} - d_{a2}u_{\mathrm{dc}}}{Z_{a2}} + \alpha^2\dfrac{e_b - u_{\mathrm{NO}} - d_{b2}u_{\mathrm{dc}}}{Z_{b2}} + \alpha\dfrac{e_c - u_{\mathrm{NO}} - d_{c2}u_{\mathrm{dc}}}{Z_{c2}}\right) \end{bmatrix} \tag{9}$$

where $\alpha = e^{j\frac{2\pi}{3}}$ is the fortescue operator, $Z_{\mathrm{kx}} = L_{\mathrm{kx}}p (k = a, b, c; x = 1, 2)$. As (9) indicates, the negative-sequence circulating current can be inhibited by suppressing the negative-sequence components in output currents or by eliminating their difference. In practical applications, the prior scheme is often preferred as it can effectively eliminate the secondary effects of negative-sequence currents.

B. Model of the ZSCC System

The ZSCC is a major concern for the converters in the parallel structure as it will distort the output currents and undermine the performance of the system. An average model of the ZSCC system under generalized unbalanced operating conditions will be favorable in analyzing the affecting factors of zero-sequence component and developing improved control algorithm. From (6), one can see that the ZSCC system is coupled with the active–reactive current system. Decoupling would be complicated and not practical. To acquire a proper mathematical model for the zero-sequence system, suppose both the active and reactive currents are well controlled with negative-sequence components eliminated. In this case, both the variations in active and reactive currents can be neglected in steady state. Thus, the ZSCC system can be simplified as

$$\begin{cases} -\dfrac{\omega L_{\sin p1}}{3}i_{d1} - \dfrac{\omega L_{\cos p1}}{3}i_{q1} + L_{m1}\dfrac{di_{z1}}{dt} = -u_{z1} \\ -\dfrac{\omega L_{\sin p2}}{3}i_{d2} - \dfrac{\omega L_{\cos p2}}{3}i_{q2} + L_{m2}\dfrac{di_{z2}}{dt} = -u_{z2} \end{cases}. \tag{10}$$

For a two converter parallel system, there is only one ZSCC flowing through the modules, namely, $i_{z1} + i_{z2} = 0$. Hence, the average model of ZSCC system can be obtained as

$$(L_{m1} + L_{m2})\frac{di_{z2}}{dt} = u_{\mathrm{Lz1}} - u_{\mathrm{Lz2}} + u_{z1} - u_{z2} \tag{11}$$

where u_{Lzx} can be calculated as

$$u_{\mathrm{Lzx}} = -\frac{\omega i_{\mathrm{dx}}L_{\sin \mathrm{px}}}{3} - \frac{\omega i_{\mathrm{qx}}L_{\cos \mathrm{px}}}{3} = \begin{bmatrix} \omega L_{\mathrm{ax}} & \omega L_{\mathrm{bx}} & \omega L_{\mathrm{cx}} \end{bmatrix} \times \begin{bmatrix} -\sin\omega t & -\cos\omega t \\ -\sin\left(\omega t - \frac{2}{3}\pi\right) & -\cos\left(\omega t - \frac{2}{3}\pi\right) \\ -\sin\left(\omega t + \frac{2}{3}\pi\right) & -\cos\left(\omega t + \frac{2}{3}\pi\right) \end{bmatrix} \begin{bmatrix} i_{\mathrm{dx}} \\ i_{\mathrm{qx}} \end{bmatrix}. \tag{12}$$

As can be observed, u_{Lzx} is the zero-sequence voltage drop on the filter inductance, essentially. Define $\Delta u_{\mathrm{Lz}} = u_{\mathrm{Lz1}} - u_{\mathrm{Lz2}}$ as the difference in inductance zero-sequence voltages between parallel modules and $\Delta d_z = d_{z1} - d_{z2}$ as the zero-sequence duty ratio difference, then the average model of ZSCC system can be calculated as

$$(L_{m1} + L_{m2})\frac{d_{\mathrm{iz2}}}{dt} = \Delta u_{\mathrm{Lz}} + \Delta d_z u_{\mathrm{dc}}. \tag{13}$$

As can be seen, the unbalance factors in filter inductance will also contribute to generating ZSCC.

III. Proposed Control Scheme for Parallel Systems Under Generalized Unbalanced Operating Conditions

A. Control of Negative-Sequence Circulating Current

To inhibit the negative-sequence circulating current, efforts should be made to suppress the negative-sequence components. Conventionally, a PI controller can be adopted in PSRF to control the active and reactive currents provided that the filter inductance and grid voltage are balanced. However, from the aforementioned, it arises that both the unbalance factors in filter inductance and grid voltage will give rise to generating negative-sequence components in the output currents and this negative-sequence component would probably result in unbalanced output currents and even more seriously, negative-sequence circulating current between the parallel modules. Unfortunately, since a negative-sequence component appears as $2\,\omega$ ac component in PSRF, the PI controller is not able to suppress it without steady-state error. To suppress the negative-sequence currents, a resonant controller can be reinforced to the traditional PI controller. The reinforced PI controller (we refer to PIR controller) can be expressed as

$$G_c(s) = k_p + \frac{k_i}{s} + \frac{k_r s}{s^2 + \omega_r s/Q + \omega_r^2} \tag{14}$$

where k_p, k_i, and k_r are the proportional, integral, and resonant gain parameters of the PIR controller, respectively, and $\omega_r = 2\,\omega$ is the resonant frequency of the controller while Q can be defined as the quality factor of the controller. The resonant function of $G_c(s)$ can provide a relatively large gain to the negative-sequence currents of $2\,\omega$ frequency in PSRF with a large Q. And it is this large gain that will effectively suppress the negative-sequence components in the active and reactive currents in steady state. As for the positive-sequence component in active and reactive currents, which is virtually dc component, the PI function of $G_c(s)$ will manage it with almost zero error in steady state.

The control block diagram of active–reactive current system is displayed in Fig. 3, and the outputs of current controllers can be calculated as

$$\begin{cases} u_{\mathrm{dx}} = -\left(k_p + \dfrac{k_i}{s} + \dfrac{k_r s}{s^2 + \omega_r s/Q + \omega_r^2}\right)(i_{\mathrm{dx\_ref}} - i_{\mathrm{dx}}) \\ \qquad +\omega L_{\mathrm{mx}} i_{\mathrm{qx}} + \tilde{e_d} \\ u_{\mathrm{qx}} = -\left(k_p + \dfrac{k_i}{s} + \dfrac{k_r s}{s^2 + \omega_r s/Q + \omega_r^2}\right)(i_{\mathrm{qx\_ref}} - i_{\mathrm{qx}}) \\ \qquad -\omega L_{\mathrm{mx}} i_{\mathrm{dx}} + \tilde{e_q} \end{cases} \tag{15}$$

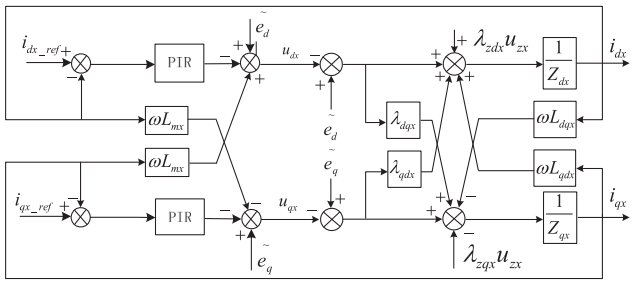

Fig. 3. Control block diagram of the active and reactive current system PSRF.

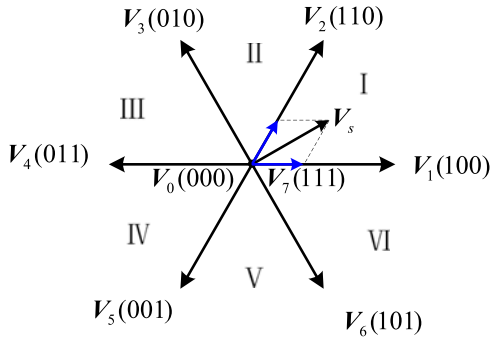

Fig. 4. Synthesis of control voltage vector with basic voltage vectors.

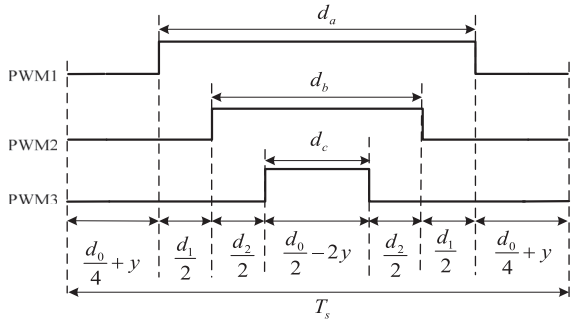

Fig. 5. Distribution of vectors with zero-vector correction variable adopted.

where $x = 1{,}2$ represent the number of converters 1 and 2, respectively.

B. Control of ZSCC With SVPWM Modulation Technique

The SVPWM modulation technique is applied in the control of three-phase PWM converters due to its advanced features including high-dc voltage utilization and less distortions in converter output currents. The control vector $\boldsymbol{V_s}$ in each PWM cycle, as illustrated in Fig. 4, is synthesized by two adjacent nonzero vectors $\boldsymbol{V_i}$ $i = 1, 2, 3, 4, 5, 6$ and two zero vectors $\boldsymbol{V_j}$ $(j = 0, 7)$. A typical vector distribution of this modulation technique when $\boldsymbol{V_s}$ lies between $\boldsymbol{V}_4$ and $\boldsymbol{V}_6$ is depicted in Fig. 5, where T_s is the time span of a PWM cycle, and d_1, d_2 represent the duty ratios of the two nonzero vectors. The two zero vectors are uniformly distributed at the beginning, end, and middle of a PWM cycle and their total duty ratio can be calculated as $d_0 = 1 - d_1 - d_2$. Another advantage of this modulation technique lies in the duration of two zero vectors can be

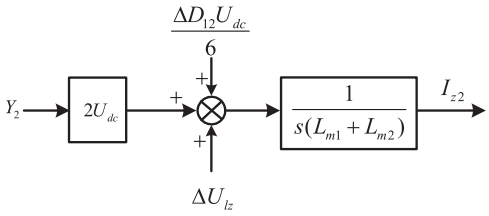

Fig. 6. ZSCC system under generalized unbalanced operating conditions.

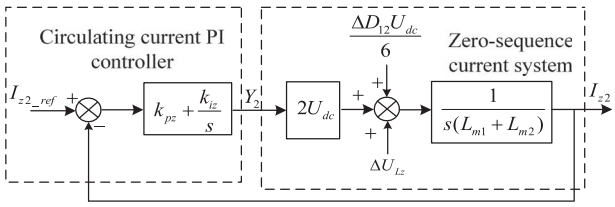

Fig. 7. Zero-sequence current loop with filter inductance unbalanced.

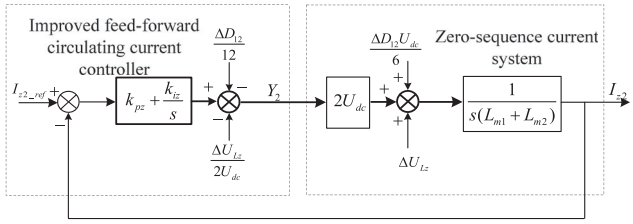

Fig. 8. Improved feed-forward circulating current control strategy.

redistributed and this advanced feature can be used to suppress the ZSCC.

As (13) indicates, the ZSCC can be suppressed by regulating the zero-sequence duty ratios of parallel modules. A control variable y can be introduced to regulate the duration of zero vectors $\boldsymbol{V}_0$ and $\boldsymbol{V}_7$, as shown in Fig. 5. The introduced control variable will redistribute the zero vectors in a PWM cycle, but would not affect the differences in phase duty ratios. Hence, the performance of active–reactive current system of each individual converter will not be affected. However, as can be noted, the zero-sequence duty ratio can be accommodated as

$$\begin{aligned} d_{\rm zx} &= (d_{\rm ax}+d_{\rm bx}+d_{\rm cx})/3 \\ &= ((d_{1x}+d_{2x}+d_{0x}/2-y_x)+(d_{2x}+d_{0x}/2-y_x) \\ &\quad +(d_{0x}/2-y_x))/3 \\ &= (3/2-d_{1x}/2+d_{2x}/2-6y_x)/3 \end{aligned} \tag{16}$$

where d_{1x} and d_{2x} $(x=1,2)$ represent the two nonzero vectors of the parallel modules. In a two converter parallel system, only one ZSCC exists. Therefore, by suppressing the ZSCC in one of the parallel modules, the zero-sequence component in output currents can be sufficiently eliminated automatically. Choose converter 2 as the target with control variable y_2, and converter 1 adopts the conventional SVPWM modulation technique, i.e., $y_1=0$. Then, the average model of the ZSCC can be obtained as

$$\frac{di_{z2}}{dt}=\frac{\Delta u_{\rm Lz}+(\Delta d_{12}/12+y_2)\cdot 2u_{\rm dc}}{(L_{m1}+L_{m2})} \tag{17}$$

where $\Delta d_{12}=(d_{21}-d_{11})-(d_{22}-d_{12})$ is the difference in nonzero vectors duty ratios.

Neglect the fluctuation in dc bus voltage, the Laplace transform of (17) can be obtained as

$$I_{z2}(s)=\frac{\Delta U_{\rm Lz}+(\Delta D_{12}/12+Y_2)2U_{\rm dc}}{s(L_{m1}+L_{m2})} \tag{18}$$

where $\Delta U_{\rm Lz}$, ΔD_{12}, and Y_2 are the Laplace transform of $\Delta u_{\rm Lz}$, Δd_{12}, and y_2, respectively. Then, the ZSCC system can be depicted as Fig. 6. Conventionally, in the modular designed converters, the unbalance factors in filter are often ignored. Thus, the outputs of active–reactive current controllers in (15) are approximately equal. As a result, the impacts of Δd_{12} and $\Delta u_{\rm Lz}$ can be neglected. Then, the average model of ZSCC can be simplified as

$$I_{z2}(s)=\frac{2Y_2U_{\rm dc}}{s(L_{m1}+L_{m2})}. \tag{19}$$

As (19) indicates, ideally the ZSCC loop of the modular designed parallel system is a first-order system independent of the active–reactive current system. Recognizing this property, a simple PI controller can be used to suppress the circulating current, and the output of the zero-axis current controller can be obtained as

$$y_2=\left(k_{\rm pz}+\frac{k_{\rm iz}}{s}\right)(i_{z2\_\rm ref}-i_{z2}) \tag{20}$$

where $i_{z2\_\rm ref}$ is the reference value of ZSCC, and $k_{\rm pz}$, $k_{\rm iz}$ are the parameters of the circulating current PI controller.

C. Control of ZSCC With Improved Feed-Forward Method

Theoretically, when the parallel modules share the same value in balanced filter inductance, the impacts of $\Delta u_{\rm Lz}$ and Δd_{12} can be ignored and relatively satisfactory circulating current suppression performance can be achieved with the traditional PI method. However, in practical applications, tolerance in inductance values of up to $\pm 10\%$ is quite common, which would contribute to unbalance in filter inductance. Unfortunately, according to (15), the unbalance factors in filter inductance will in return give rise to different output ac voltages for the parallel converters. Moreover, as (12) indicates, different inductance zero-sequence voltages will probably be produced. Based on the analysis aforementioned, the angular frequency of $\Delta u_{\rm Lz}$ is ω, just the angular frequency of grid fundamental component, which is usually lower than the bandwidth of ZSCC control system. In a word, as depicted in Fig. 7, both $\Delta u_{\rm Lz}$ and Δd_{12} will cause significant disturbances to the ZSCC system. Consequently, the suppressing performance of PI controller would be deteriorated.

To overcome the disadvantage of traditional PI method in suppressing ZSCC and eliminate the impacts caused by $\Delta u_{\rm Lz}$ and Δd_{12}, a feed-forward strategy on the basis of traditional PI method is proposed as shown in Fig. 8. The feed-forward quantity $\Delta d_{12}/12$ and $\Delta u_{\rm Lz}/2u_{\rm dc}$ are used to reject the disturbances caused by Δd_{12} and $\Delta u_{\rm Lz}$, respectively. With the

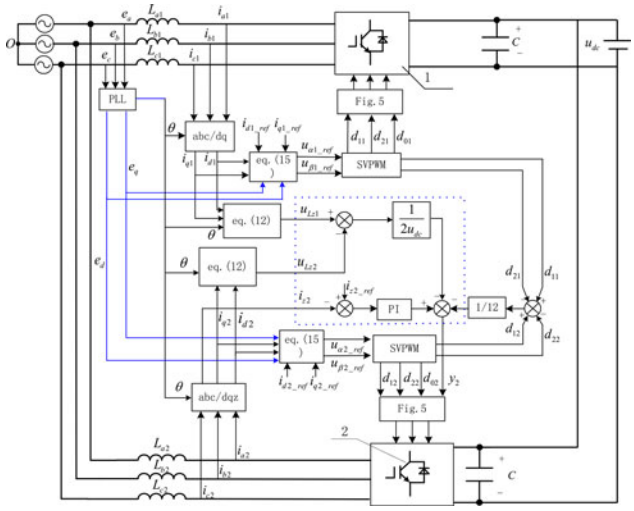

Fig. 9. System block diagram of the parallel three phase PWM structure with improved feed-forward circulating current controller.

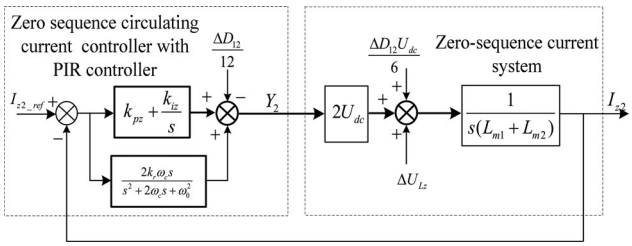

Fig. 10. Proposed circulating current control strategy with PIR controller.

proposed feed-forward control strategy, the circulating current control variable can be obtained as

$$y_2 = \left(k_{\rm pz} + \frac{k_{\rm iz}}{s}\right)(i_{z2\_\rm ref} - i_{z2}) - \frac{\Delta d_{12}}{12} - \frac{\Delta u_{\rm lz}}{2u_{\rm dc}}. \quad (21)$$

Theoretically, the disturbances in ZSCC system can be effectively rejected and better suppression performance can be achieved.

The system control block diagram of the proposed control scheme for the parallel system is shown in Fig. 9. The active and reactive currents are controlled by PIR controllers which can effectively inhibit the negative-sequence components in output currents and suppress the negative-sequence circulating current. It should be noted that the outputs $u_{\alpha x\_\rm ref}$ and $u_{\beta x\_\rm ref}$ are the Clarke transformation of $u_{\rm dx}$ and $u_{\rm qx}$, respectively. And it is worth mentioning that a notch filter is used in the phase-locked loop to trace the phase angle of positive-sequence component in the grid voltage. The transfer function of the notch filter is

$$F(s) = \frac{s^2 + \omega_n^2}{s^2 + \omega_n / Q_f + \omega_n^2} \quad (22)$$

where $\omega_n = 2\,\omega(\omega$ is the grid fundamental angular frequency) and $Q_f = 10$.

The ZSCC control block is displayed in the shaded area. The ZSCC in converter 2 is suppressed to eliminate the zero-sequence component in output currents of the parallel modules. The difference between i_{z2} and its reference value is fed into the PI controller. Meanwhile, the feed-forward quantity of Δd_{12} is obtained by calculating the time durations of two nonzero vectors t_{1x} and t_{2x} $(x = 1, 2)$ in each PWM cycle as $d_{1x} = t_{1x}/T_s$, $d_{2x} = t_{2x}/T_c$. Simultaneously, (12) is used to obtain another feed-forward quantity $\Delta u_{\rm lz}/2u_{\rm dc}$. Then, the ZSCC control variable y_2 is utilized to adjust the zero-sequence duty ratio of converter 2 by redistributing the time duration of zero vectors in each PWM cycle.

Fig. 11. Structure of parallel system. (a) Paralleled converters and filter inductance. (b) TMS320f2812 DSP based control board.

D. Control of ZSCC With PIR Method

Because the disturbances in ZSCC system caused by unbalance factors in filter inductance should be calculated in feed-forward method, so the improved feed-forward circulating current controller is sensitive to parameters of filter inductances.

From (12), the disturbances caused by unbalance filter inductances can be expressed

$$\begin{aligned}\Delta u_{\rm lzx} = & -\omega i_d(\Delta L_a \sin\omega t + \Delta L_b \sin(\omega t - 2\pi/3) + \Delta L_c \sin(\omega t \\ & + 2\pi/3)) - \omega i_q(\Delta L_a \cos\omega + \Delta L_b \cos(\omega t - 2\pi/3) \\ & + \Delta L_c \cos(\omega t + 2\pi/3)) \end{aligned} \quad (23)$$

where $\Delta L_a = L_{a1} - L_{a2}$, $\Delta L_b = L_{b1} - L_{b2}$, $\Delta L_c = L_{c1} - L_{c2}$.

In steady state, the currents in dq frame are constant, so it can be seen that the disturbances caused by unbalance filter inductances is the fluctuation in grid frequency. So, the fluctuation in grid frequency can be suppressed by the resonance controller. Based on the method in [26], the ZSCC controller is as follows:

$$y_2 = \left(k_{\rm pz} + \frac{k_{\rm iz}}{s} + \frac{2k_r\omega_c s}{s^2 + 2\omega_c s + \omega_0^2}\right)(i_{z2\_\rm ref} - i_{z2}) - \frac{\Delta d_{12}}{12}. \quad (24)$$

The both proposed scheme can be applied to the three-phase PWM converter parallel system which contains communication line. Whereas communication synchronization and the accurate information of filter inductance in parallel modules are the key factors in ensuring the circulating current suppression performance.

IV. Experimental Results

To verify the validity of the theoretical analysis and the effectiveness of the proposed scheme, a prototype system (see Fig. 11) with two-paralleled converters is constructed with some specific parameters as shown in Table I. The adopted active switches are IGBT (FF1400R21P4). The proposed scheme is

TABLE I
EXPERIMENTAL PARAMETERS

DC bus voltage	450 V
AC line voltage	200 V
Unbalanced ac voltage	$U_{ab} = 200$ V, $U_{bc} = 173$ V, $U_{ca} = 100$ V
Fundamental frequency (Grid)	50 Hz
Current reference	$I_{d1\_ref} = I_{d2\_ref} = 10$ A (rms), $I_{q1\_ref} = I_{q2\_ref} = 0$
Switching frequency	5 kHz
Sampling frequency	10 kHz
Inductor of converter1	$L_{a1} = L_{b1} = L_{c1} = 6$ mH
Inductor of converter2	$L_{a2} = 6$ mH, $L_{b2} = 4$ mH, $L_{c2} = 2$ mH

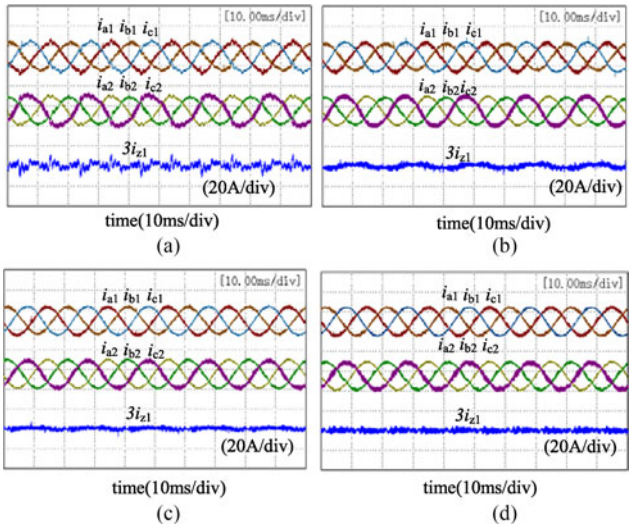

Fig. 12. Experimental results in balanced grid voltage condition.

implemented in a TMS320F2812 DSP with the synchronous PWM. The unbalanced voltage is generated by a multiple tap transformer.

Four different ZSCC control methods are compared in the experiments. Method-1 is conventional PI controller. Method-2 is PI and feed-forward control methods in [26]. Method-3 is PI and improved feed-forward control proposed in this paper, in which the disturbances caused by unbalance filter inductance are suppressed by feed-forward. Method-4 is proposed PIR and feed-forward control methods, in which the disturbances caused by unbalance filter inductance are suppressed by resonance controller. In order to illustrate the validity of proposed method, only the situation of balanced reference output currents is considered.

Fig. 12 shows the experimental results in balanced grid voltage condition. In Fig. 12(a), active, reactive, and ZSCC were controlled by the traditional PI method. In Fig. 12(b), active and reactive current were controlled by PIR controller, circulating current was controlled by the PI and zero-sequence duty ratio difference feed-foreword method. Obviously the frequency of the ZSCC is equal to the fundamental frequency of the grid voltage. With PIR controller, the output currents were nearly balanced. With the PI and zero-sequence duty ratio difference feed-foreword method, the circulating current was suppressed, but the difference in inductance zero-sequence voltages will cause ripple in circulating current. Fig. 12(c) shows the waveform of Method-3 (Fig. 8). The proposed method is PI plus

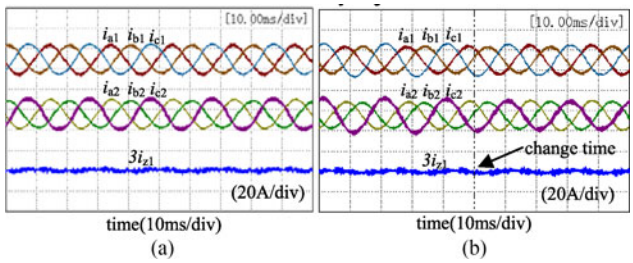

Fig. 13. Experimental results with circulating current controlled by Method-3 in different condition. (a) Active and reactive current were controlled by PI controller in grid voltage balanced condition. (b) Active and reactive current were controlled from PI controller to PIR controller in grid voltage unbalanced condition.

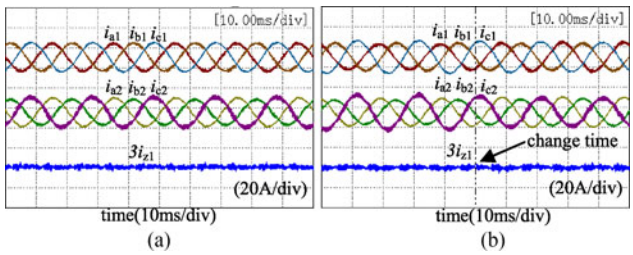

Fig. 14. Experimental results with circulating current controlled by Method-4 in different condition. (a) Active and reactive current were controlled by PI controller in grid voltage balanced condition. (b) Active and reactive current controller changed from PI controller to PIR controller in grid voltage unbalanced condition.

zero-sequence duty ratio difference and difference in inductance zero-sequence voltages feed foreword. With the proposed method, the amplitude of the circulating current impact can be decreased, compared to the method proposed in [26] (PI and zero-sequence duty ratio difference feed-foreword method), because of the feed foreword of the difference in inductance zero-sequence voltages. Fig. 12(d) shows the waveform of Method-4 (Fig. 10). As shown, improved suppression performance can be achieved with the proposed as the disturbances caused by unbalance factors in filter inductance can be effectively rejected.

Figs. 13 and 14 show the experimental results with proposed method. As shown, the filter inductance unbalance will cause significant disturbances to the output current. The active and reactive current PI controller cannot realize controlling negative-sequence currents without steady-state error, resulting in unbalanced output currents in the parallel modules. The negative-sequence components will be increased in unbalanced grid voltage condition. The negative-sequence components can be eliminated by active and reactive current PIR controller. Table II shows the negative current of paralleled converters by different circulating current controllers (active–reactive current controller and ZSCC controller). The performance of proposed circulating control method was good in different condition.

Fig. 15 presents the experimental results of current step response in unbalanced grid voltage condition. As the figure indicates the paralleled converters can be running under different reference-current dynamic conditions. The reliability and robustness of the parallel system can be improved in unbalanced filter and grid voltage condition. The proposed method can also

TABLE II
NEGATIVE SEQUENCE CURRENTS (RMS) OF PARALLELED CONVERTERS IN DIFFERENT CONDITION (A)

	Grid voltage balanced				Grid voltage unbalanced			
Active and reactive current controller	PI		PIR		PI		PIR	
Converter number	Cov.1	Cov.2	Cov.1	Cov.2	Cov.1	Cov.2	Cov.1	Cov.2
Zero-sequence controller Method-1	0.32	1.22	0.35	0.62	1.37	2.27	0.36	0.66
Zero-sequence controller Method-2	0.40	1.03	0.30	0.56	1.35	2.34	0.27	0.58
Zero-sequence controller Method-3	0.33	0.97	0.22	0.31	1.47	2.40	0.28	0.52
Zero-sequence controller Method-4	0.40	1.10	0.35	0.65	1.53	2.37	0.27	0.46

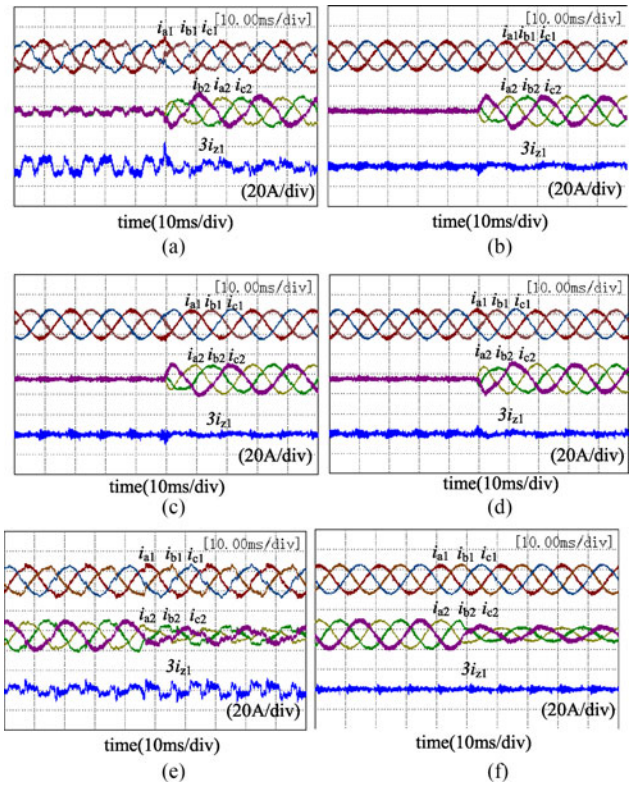

Fig. 15. Experimental results of current step response in unbalanced grid voltage condition.

be used when the parallel converter operated with different currents.

Table III shows ZSCCs (rms) in different condition with active and reactive current PIR controller. It can be seen that the ZSCC can be suppressed better with proposed Method-3 and Method-4, compared to the conventional PI (Method-1) and Method-2 proposed in [26]. The performance of Method-4 is better than Method-3 because Method-4 does not rely on inductor parameters.

TABLE III
ZERO-SEQUENCE CIRCULATING CURRENTS (RMS) IN DIFFERENT CONDITION WITH ACTIVE AND REACTIVE CURRENT PIR CONTROLLER (A)

	Grid voltage balanced	Grid voltage unbalanced
Method-1	3.226	3.632
Method-2	1.883	2.0
Method-3	1.456	1.604
Method-4	1.364	1.407

V. CONCLUSION

This paper has proposed a new scheme to control parallel three-phase PWM converters under generalized unbalanced conditions. The unbalance factors in filter inductance will give rise to negative-sequence components in output currents and cause disturbances to the ZSCC system. Consequently, circulating currents would be generated and the output currents of parallel modules would be distorted. By suppressing the negative-sequence components in output currents, the negative-sequence circulating current can be effectively inhibited. Moreover, the disturbances in ZSCC system can be effectively rejected by the proposed feed-forward strategy or the PIR controller. Improved circulating currents suppression performance can be achieved, and as a result, the distortions in output currents of parallel modules could be greatly reduced. Experimental results validate the performance and effectiveness of the proposed scheme.

REFERENCE

[1] P. K. Goel, B. Singh, S. S. Murthy, and N. Kishore, "Parallel operation of DFIGs in three-phase four-wire autonomous wind energy conversion system," *IEEE Trans. Ind. Appl.*, vol. 47, no. 4, pp. 1872–1883, Jul./Aug. 2011.

[2] M. F. Schonardie *et al.*, "Control of the active and reactive power using dq0 transformation in a three-phase grid-connected PV system," in *Proc. IEEE 21st Int. Symp. Ind. Electron.*, 2012, pp. 264–269.

[3] M. Borrega, L. Marroyo, R. Gonz´alez, J. Balda, and J. L. Agorreta, "Modeling and control of a master—Slave PV inverter with N-paralleled inverters and three-phase three-limb inductors," *IEEE Trans. Power Electron.*, vol. 28, no. 6, pp. 2842–2855, Jun. 2013.

[4] T. Itkonen, J. Luukko, A. Sankala, and T. Laakkonen,"Modeling and analysis of the dead-time effects in parallel PWM two-level three-phase voltage-source inverters," *IEEE Trans. Power Electron.*, vol. 24, no. 11, pp. 2446–2455, Nov. 2009.

[5] T.-P. Chen, "Dual-modulator compensation technique for parallel inverters using space-vector modulation," *IEEE Trans. Ind. Electron.*, vol. 56, no. 8, pp. 3004–3012, Aug. 2009.

[6] S. Ogasawara, J. Takagaki, H. Akagi, and A. Nabae, "A novel control scheme of a parallel current-controlled PWM inverter," *IEEE Trans. Ind. Appl.*, vol. 28, no. 5, pp. 1023–1030, Sep./Oct. 1992.

[7] K. Xing, F. C. Lee, D. Boroyevich, Z. Ye, and S. K. Mazumder,"Interleaved PWM with discontinuous space-vector modulation," *IEEE Trans. Power Electron.*, vol. 14, no. 5, pp. 906–917, Sep. 1999.

[8] T.-P. Chen, "Zero-sequence circulating current reduction method for parallel HEPWM inverters between AC bus and DC bus," *IEEE Trans. Ind. Electron.*, vol. 59, no. 1, pp. 290–300, Jan. 2012.

[9] C.-C. Hou, "A multicarrier PWM for parallel three-phase active front-end converters," *IEEE Trans. Power Electron.*, vol. 28, no. 6, pp. 2753–2759, Jun. 2013.

[10] Z. Ye, D. Boroyevich, and F. C. Lee, "Paralleling non-isolated multi-phase PWM converters," in *Proc. IEEE Ind. Appl. Conf. Rec.*, 2000, pp. 2333–2439.

[11] Z. Ye, D. Boroyevich, J.-Y. Choi, and F. C. Lee, "Control of circulating current in two parallel three-phase boost rectifiers," *IEEE Trans. Power Electron*., vol. 17, no. 5, pp. 609–615, Sep. 2002.

[12] S. K. Mazumder, "Continuous and discrete variable structure controls for parallel three-phase boost rectifier," *IEEE Trans. Ind. Electron.*, vol. 52, no. 2, pp. 340–354, Apr. 2005.
[13] M. Reyes, P. Rodriguez, S. Vazquez, A. Luna, R. Teodorescu, and J. M. Carrasco, "Enhanced decoupled double synchronous reference frame current controller for unbalanced grid-voltage conditions," *IEEE Trans. Power Electron.*, vol. 27, no. 9, pp. 3934–3943, Sep. 2012.
[14] S. Vazquez, J. A. Sanchez, M. R. Reyes, J. I. Leon, and J. M. Carrasco, "Adaptive vectorial filter for grid synchronization of power converters under unbalanced and/or distorted grid conditions," *IEEE Trans. Ind. Electron.*, vol. 61, no. 3, pp. 1355–1367, Mar. 2014.
[15] F. Nejabatkhah, Y. W. Li, and B. Wu, "Control strategies of three-phase distributed generation inverters for grid unbalanced voltage compensation," *IEEE Trans. Power Electron.*, vol. 31, no. 7, pp. 52287–5241, Jul. 2016.
[16] L. Meng *et al.*, "Distributed voltage unbalance compensation in islanded microgrids by using a dynamic consensus algorithm," *IEEE Trans. Power Electron.*, vol. 31, no. 1, pp. 827–837, Jan. 2016.
[17] Y. A.-R. I. Mohamed, "Mitigation of dynamic, unbalanced, and harmonic voltage disturbances using grid-connected inverters with LCL filter," *IEEE Trans. Ind. Electron.*, vol. 58, no. 9, pp. 3914–3924, Sep. 2011.
[18] C.-T. Pan and Y.-H. Liao, "Modeling and coordinate control of circulating currents in parallel three-phase boost rectifiers," *IEEE Trans. Ind. Electron.*, vol. 54, no. 2, pp. 825–838, Apr. 2007.
[19] C.-T. Pan and Y.-H. Liao, "Modeling and control of circulating currents for parallel three-phase boost rectifiers with different load sharing," *IEEE Trans. Ind. Electron.*, vol. 55, no. 7, pp. 2776–2785, Jul. 2008.
[20] J.-K. Ji and S.-K. Sul, "Operation analysis and new current control of parallel connected dual converter system without interphase reactors," in *Proc. IEEE 25th Annu. Conf. Ind. Electron. Soc.*, 1999, pp. 235–240.
[21] R. Inzunza, T. Sumiya, Y. Fujii, and E. Ikawa, "Parallel connection of grid-connected LCL inverters for MW-scaled photovoltaic systems," in *Proc. Int. Power Electron. Conf.*, Jun. 2010, pp. 1988–1993.
[22] F. Ueda, K. Matsui, M. Asao, and K. Tsuboi, "Parallel-connections of pulsewidth modulated inverters using current sharing reactors," *IEEE Trans. Power Electron.*, vol. 10, no. 6, pp. 673–679, Nov. 1995.
[23] X. Yuan, W. Merk, and H. Stemmler, "Stationary-frame generalized integrators for current control of active power filters with zero steady-state error for current harmonics of concern under unbalanced and distorted operating conditions," *IEEE Trans. Ind. Appl.*, vol. 38, no. 2, pp. 523–532, Mar./Apr. 2002.
[24] D. G. Holmes, T. A. Lipo, B. P. McGrath, and W. Y. Kong, "Optimized design of stationary frame three phase ac current regulators AC current regulators," *IEEE Trans. Power Electron.*, vol. 24, no. 11, pp. 2417–2426, Nov. 2009.
[25] A. Kuperman, "Proportional-resonant current controllers design based on desired transient performance," *IEEE Trans. Power Electron.*, vol. 30, no. 10, pp. 5341–5345, Oct. 2015.
[26] X. Zhang, J. Chen, Y. Ma, Y. Wang, and D. Xu, "Bandwidth expansion method for circulating current control in parallel three-phase PWM converter connection system," *IEEE Trans. Power Electron.*, vol. 29, no. 12, pp. 6847–6856, Dec. 2014.
[27] P. D. Antoszczuk and R. G. Retegui, "Characterization of steady-state current ripple in interleaved power converters under inductance mismatches," *IEEE Trans. Power Electron.*, vol. 29, no. 4, pp. 1840–1849, Apr. 2014.
[28] J. S. S. Prasad and G. Narayanan, "Minimization of grid current distortion in parallel-connected converters through carrier interleaving," *IEEE Trans. Ind. Electron.*, vol. 61, no. 1, pp. 76–91, Jan. 2014.
[29] T.-P. Chen, "Dual-modulator compensation technique for parallel inverters using space-vector modulation," *IEEE Trans. Ind. Electron.*, vol. 56, no. 8, pp. 3004–3012, Aug. 2009.

Xueguang Zhang (M'13) was born in Heilongjiang, China, in 1981. He received the B.S., M.S., and Ph.D. degrees in electrical engineering from the Harbin Institute of Technology, Harbin, China, in 2003, 2005, and 2010, respectively.

Since 2015 he has been an Associate Professor in the Department of Electrical and Engineering, Harbin Institute of Technology. His current research interests include distributed generation and renewable energy conversion systems.

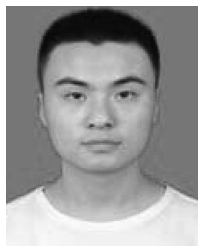

Zhichao Fu was born in Shandong, China, in 1992. He received the B.S. degree in electrical engineering from Southwest Jiaotong University, Chengdu, China, in 2016. He is currently working toward the M.S. degree from the Harbin Institute of Technology, Harbin, China.

His current research interests include grid-connected inverter systems modeling and stability analysis.

Yi Xiao was born in Hubei, China, in 1992. She received the B.S. degree from the Department of Hydropower and Information Engineering, Huazhong University of Science and Technology, Wuhan, China, in 2015. She is currently working toward the M.S. degree from the Department of Electrical Engineering, Harbin Institute of Technology, Harbin, China.

Her current research interests include grid-connected inverter systems and modern control technologies.

Gaolin Wang (M'13) received the B.S., M.S., and Ph.D. degrees in electrical engineering from the Harbin Institute of Technology, Harbin, China, in 2002, 2004, and 2008, respectively.

In 2009, he joined the Department of Electrical Engineering, Harbin Institute of Technology as a Lecturer, where he has been a Professor of Electrical Engineering since 2014. From 2009 to 2012, he was a Postdoctoral Fellow in Shanghai STEP Electric Corporation. He has authored more than 50 technical papers published in journals and conference proceedings. He is the holder of ten Chinese patents. His current major research interests include ac motor drives, position sensorless control, and digital control of power converters.

Dianguo Xu (M'97–SM'12) was born in Heilongjiang, China, in 1960. He received the B.S. degree in control engineering from the Harbin Shipbuilding Engineering Institute, Harbin, China, in 1981, and the M.S. and Ph.D. degrees in electrical engineering from the Harbin Institute of Technology, Harbin, in 1984 and 1990, respectively.

Since 1994 he has been a Professor with the Department of Electrical Engineering, Harbin Institute of Technology. His current research interests include robotics, lighting electronics, power quality mitigation, consumer electronics, power electronics, and motor drives.

Dr. Xu is a Member of the China Electrotechnical Society and China Power Supply Society.